Fisher Space Systems, LLC

Space Track Launch System
Flexible Ribbon Model

by
Jerry F. Fisher

1. Introduction

The Space Track Launch System (STLS) is a two stage launch system. The first stage is a tall tower with rotating ribbons (Fisher, J.F., 2011). The tower (figure 1) is from 100-150 km in height. At the top of the tower, there is a rotating truss which supports four ribbons (two ribbons from each end of the truss) made of high strength fiber composites. Counterweights (CW) (Fisher, J.F., 2010) are attached to the end of each ribbon.

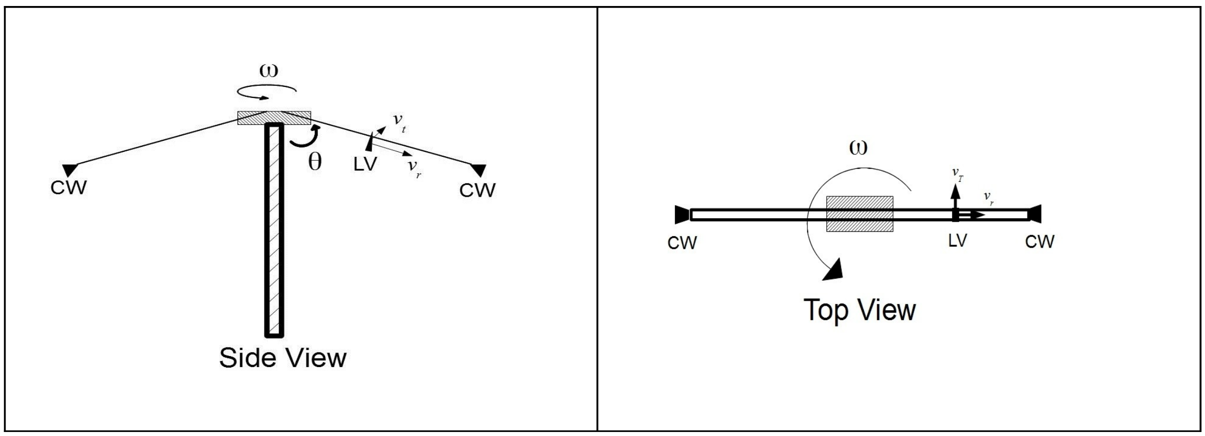

Figure 1. Space Track Launch System

The second stage is a liquid fueled launch vehicle (LV) designed to launch from the STLS (Fisher, J.F., 2009). The launch vehicle attaches to an ejector which is attached to an overcarriage (Fisher, J.F., 2010). The overcarriage has four tapered wheels which rest on top of the ribbon. The overcarriage and launch vehicle travel down the ribbon and are accelerated by the centrifugal force resulting from the distance from the axis of rotation and by the contact force (Coriolis force) provided by the rotating ribbon. At a predetermined point along the ribbon, the ejector fires and the launch vehicle detaches from the overcarriage and ribbon. The liquid propellant rocket engines ignite and the second stage proceeds into orbit. The overcarriage returns to the launch site to be refurbished and reused.

The system is unique for several reasons. First, the first stage is all electric and can be used up to three times a day. The electric motors restore rotational kinetic energy to the ribbons in approximately 8 hours. Second, the launch vehicle launches from a point along the ribbon as opposed to being released from the end of the ribbon as in previous concepts. For a 80 ton launch vehicle, launching from the end of the ribbon produces a compressive shock wave that will destroy the ribbon and damage the tower. When launched from the middle of the ribbon, the additional force on the ribbon is several orders of magnitude less than the tension in the ribbon. As such, the impulse from launch is absorbed by the ribbon and counterweights and the stress on the tower is greatly reduced. Finally, the second stage launch vehicle and overcarriage are reusable making the STLS a completely reusable launch system.

The original ribbon model for the second generation STLS assumes a rigid (stiff) ribbon. This is a valid assumption for the second generation system when using carbon nanotube ribbons and a 200 ton counterweight. The material tensile strength, modulus of elasticity, and mass density of a carbon nanotube ribbon is such that the ribbon is approximately a straight line from the tower to the counterweight (as shown in figure 1). Therefore, each mass segment is at a constant angle with respect to the axis of rotation. It is this angle along with the angular velocity that determine the area and mass of each mass segment and thus, the total mass of the ribbon.

Using presently available materials for the first generation system invalidates the original assumption. The ribbon is no longer a straight line but has a definite curvature (figure 4). The angle with respect to the axis of rotation of each mass segment varies slightly. This effects the area and mass of each mass segment and thus, has a substantial effect on the total mass of the ribbon. This paper introduces a new flexible model for the ribbon.

2. Flexible Ribbon Model (Theory)

For the flexible ribbon model, several new assumptions are needed. First, assume that the ribbon is made of point masses connected by a lightweight unbreakable string (figure 2). Each point mass represents a 100 m ribbon segment. Each ribbon segment has a uniform mass. The mass of the new ribbon segment is determined by the tension in the string and the properties of the ribbon material. The new mass is added to the old mass and the process is repeated. In this fashion, the total mass of the ribbon is determined. The analysis begins at the counterweight.

Assume that the counterweight is attached to the axis of rotation by a lightweight unbreakable string. The arrangement is similar to a conical pendulum (figure 3). The tension in the string is given by,

$$T_{cw} = \sqrt{[(m_{cw} g)^2 + (m_{cw} a_c)^2]}$$

where a_c is the centripetal acceleration given by $\omega^2 r_{cw}$. The angle the first string makes with the axis of rotation is given by,

$$\cos\theta_{cw} = \frac{m_{cw} g}{T_{cw}}$$

Initially, an educated guess is required for the angular velocity, ω, and the radius, r_{cw}. The educated guess is given by the equations from the rigid model theory (Fisher, J.F., 2011). Once the tension in the first string is known, the mass of the first ribbon segment adjacent to the counterweight is determined from the material properties of the ribbon, i.e. the tensile strength and the mass density. The mass of the new segment is added to the mass of the counterweight. The radius from the axis of rotation of ribbon segment #1 is determined by subtracting $\Delta l_r \sin\theta_{cw}$ from the radius of the counterweight, r_{cw},, as shown in figure 2 below.

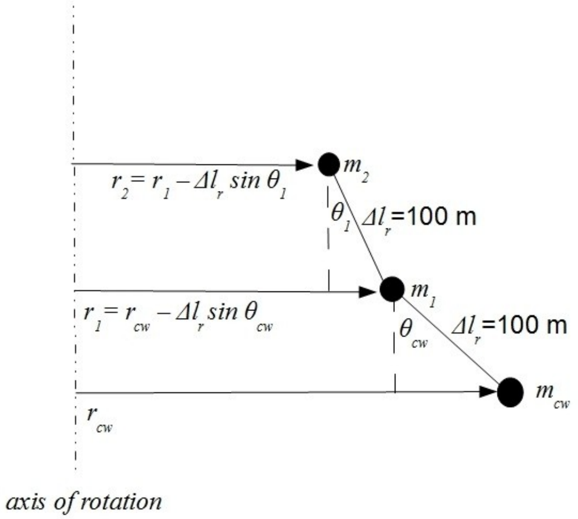

Figure 2. Mass Segments

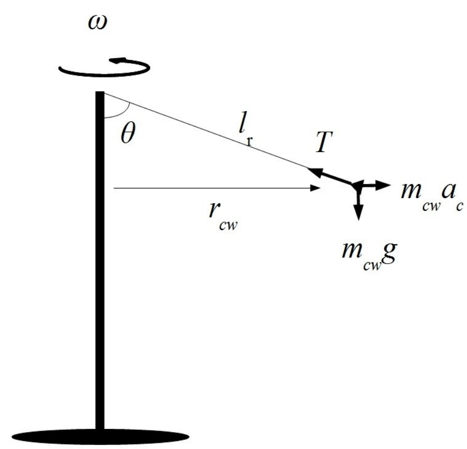

Figure 3. Conical Pendulum

The tension in the second string attaching ribbon segment #1 with ribbon segment #2 is given by,

$$T_1 = \sqrt{[(m_{cw} + m_1)\,g]^2 + (m_{cw} r_{cw} + m_1 r_1)^2\,\omega^4}$$

and in general the tension from all the ribbon segments is given by,

$$T_n = \sqrt{[(m_{cw} + m_1 + m_2 + ... + m_n)\,g]^2 + (m_{cw} r_{cw} + m_1 r_1 + m_2 r_2 + ... + m_n r_n)^2\,\omega^4}$$

and the angle the second string makes with the axis of rotation is given by,

$$\cos\theta_1 = \frac{(m_{cw} + m_1)\,g}{T_1}$$

and in general the final angle at the tower truss is given by,

$$\cos\theta_n = \frac{(m_{cw} + m_1 + m_2 + ... + m_n)\,g}{T_n}$$

The procedure is carried out until the mass of all the ribbon segments are determined. At the end of the procedure, the radius from the axis of rotation of the final ribbon segment must fall within the length of the rotating truss. If not, a new radius for the counterweight is entered and the procedure is repeated. A spreadsheet is set up to handle the calculations and is shown in the appendix.

3. Flexible Ribbon Model (Results)

Figure 4 below is a graphical representation of the ribbon for a tower height of 100 km, a ribbon length of 100 km, and a counterweight mass of 35 ton. The ribbon material is Spectra® 2000 with a density of 970 kg/m^3, an ultimate tensile strength of 3.4 GPa, and a working tensile strength of 1.14 GPa. By plotting the altitude of each ribbon segment versus its radius from the axis of rotation, the curvature of the ribbon is well represented.

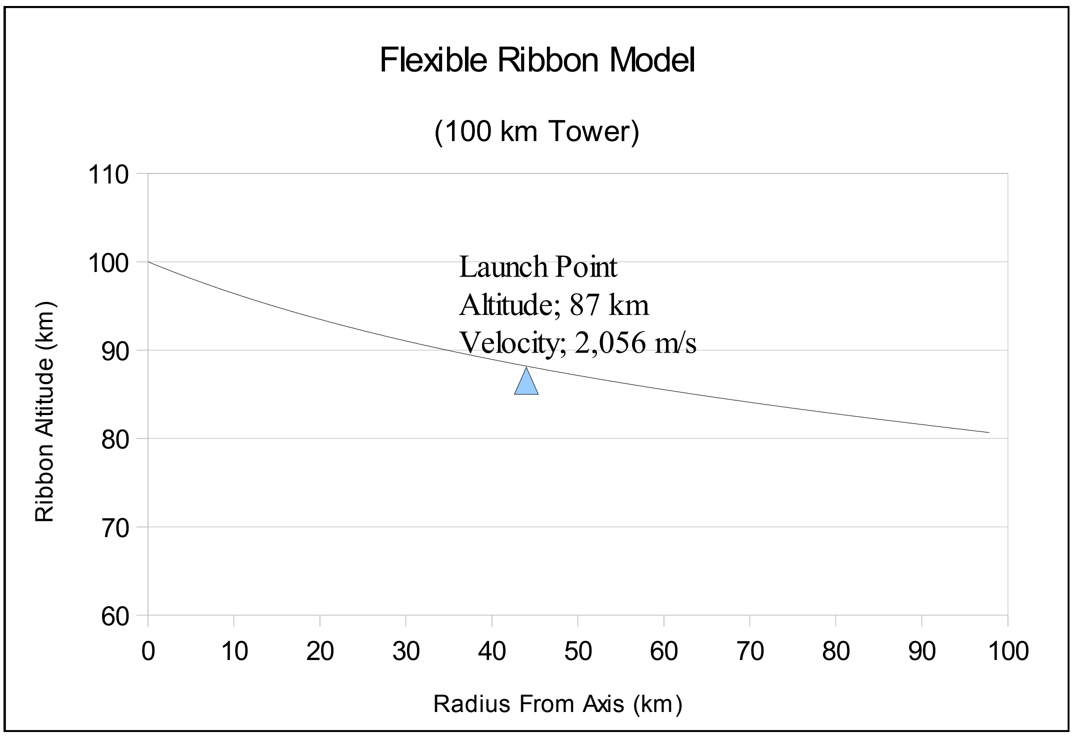

Figure 4. Curvature of Ribbon

Of particular note is the angle, θ, each ribbon segment makes with the axis of rotation at the tower and at the counterweight. The angle changes from 85° at the tower to 65° at the counterweight. The angle has an impact on the tension and thus the mass of the ribbon and also on the launch velocity.

4. Launch Velocity and Altitude

The launch velocity (figure 5) of the second stage launch vehicle consist of a radial component and a tangential component. The radial velocity is determined by using the equations of motion with the radial acceleration kept constant over the length of the ribbon segment. The tangential velocity is a product of the angular velocity of the ribbon and the distance from the axis of rotation. Fortunately, all of the necessary information is obtained from the flexible ribbon model. From the equations of motion,

Equations of Motion	Radial Acceleration and Launch Velocity
$v_{rf}^2 = v_{ri}^2 + 2\,a_r\,\Delta x$	$a_r = g\cos\theta + \omega^2 r\sin\theta$
$t = \dfrac{(v_{rf} - v_{ri})}{a_r}$	$v_t = \omega r$
	$v_L = \sqrt{(v_r^2 + v_t^2)}$

where Δx is the length of the ribbon segment equal to 100 m, t is the time interval over the ribbon segment, g is the gravitational acceleration at 100 km altitude equal to 9.5 m/s^2, and ω is the angular velocity of the ribbon equal to 2.95 x 10^{-2} rad/sec. A spreadsheet is used to handle the calculations and is included in the appendix.

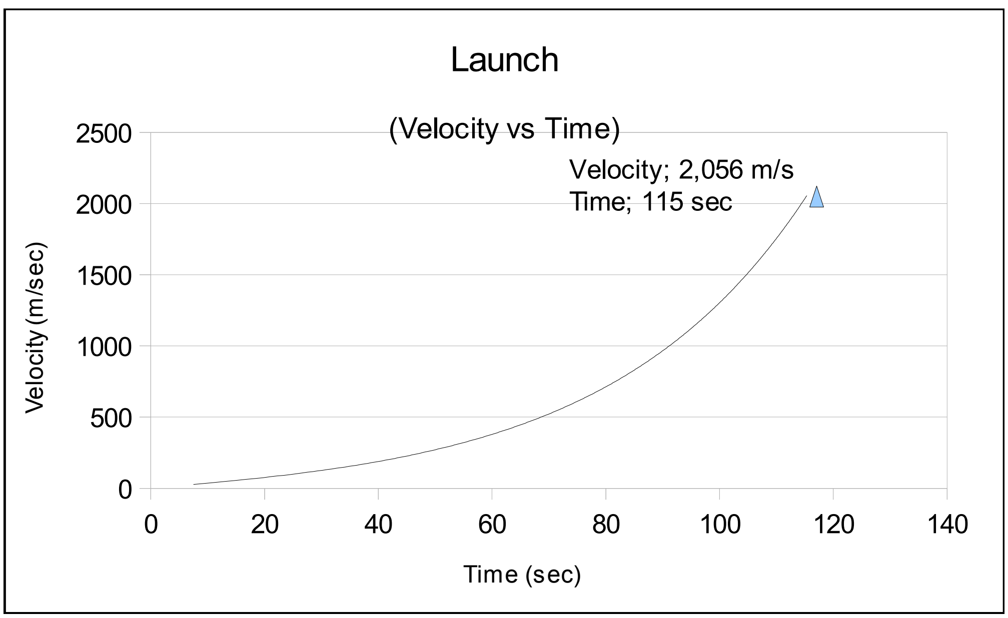

Figure 5. Launch Velocity vs Time

5. Acceleration Experienced by the Pilot

The launch velocity is limited by the acceleration experienced by the pilot. In a first generation system, the pilot is assumed to be a rugged individual into extreme sports. For example, the maximum turn in an aerobatic plane or fighter jet produces an acceleration of 9-12g (Wikipedia, 2012). Therefore, for the first generation second stage launch vehicle, the maximum acceleration is set at 10g or 98.1 m/s^2. The total acceleration experienced by the pilot (figure 6) is the vector sum of the gravitational, centripetal, and Coriolis acceleration and is given by,

$$a_t = \sqrt{(g^2 + (\omega^2 r)^2 + (2\omega v_r)^2)}$$

The acceleration experienced by the pilot is not a constant 10g acceleration. As shown in figure 6, the acceleration increase exponentially from approximately 6g to 10g in about 15 seconds. Also, note that most cargo can take a higher g loading. Therefore, higher orbits or larger payloads can be achieved with the same type of launch vehicle.

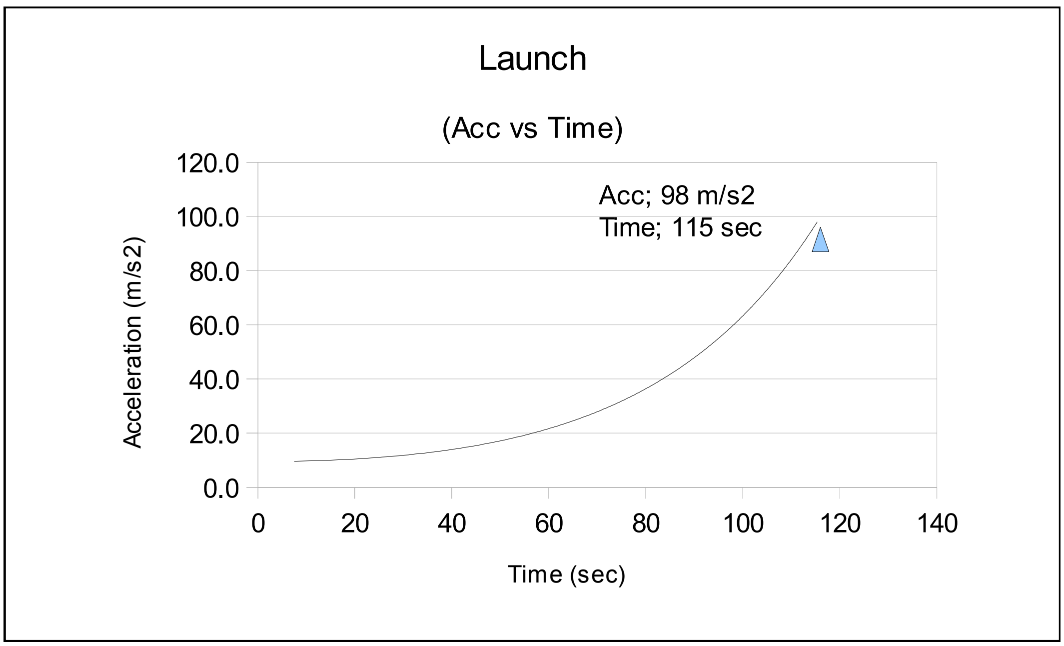

Figure 6. Acceleration Experienced by the Pilot

6. Kinetic Energy of Rotation

The ribbons kinetic energy of rotation (KER) is over 10^{12} J. For a 35 ton spacecraft, the kinetic energy at launch is approximately 10^{11} J. With 5 MW of power available at the ribbon center of mass, it would take approximately 5-6 hours to restore the KER.

With two ribbons, the first generation STLS could launch a second spacecraft 110 seconds later. Assuming two more spacecraft are prepped and ready to go at the base of the tower (similar to aircraft on a taxiway waiting to takeoff), it would most likely take 7-8 hours to get the two spacecraft up the tower and ready for launch. Therefore, the maximum capability of launch is up to six spacecraft a day. This represents a maximum of 1,200 kg of cargo or 6 pilots a day.

7. Ribbon Deflection at Launch

Due to the Coriolis force on the launch vehicle and overcarriage and the fact that the ribbon is fixed at the tower and free at the counterweight, the ribbon will be displaced several thousand meters at the point of launch. This is very similar to the dynamic stability of the ribbon for the space elevator (de Vries, J., 2006). From the Delft University of Technology final report, the displacement due to the Coriolis force is shown in figure 7 below and is given by,

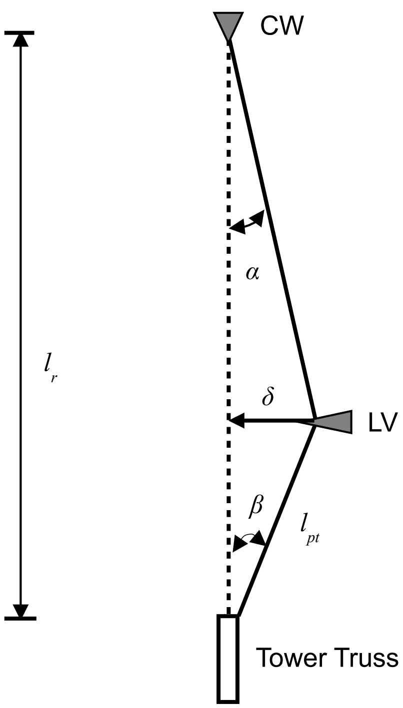

$$\delta_{max} = l_{pt}\left(1 - \frac{l_{pt}}{l_r}\right)\left[\frac{(2\,\omega\, v_L\, m_{LV})}{T_{pt}}\right]$$

Figure 7. Displacement due to Coriolis Force

where δ_{max} is the maximum displacement of the ribbon just prior to launch, l_{pt} is the launch point along the ribbon, l_r is the ribbon length, ω is the angular velocity of the ribbon, v_L is the velocity at launch, m_{LV} is the mass of the launch vehicle and overcarriage, T_{pt} is the tension in the ribbon at the launch point, α is the displacement angle at the counterweight, and β is the displacement angle at the tower truss. From the example above, the maximum deflection of the ribbon at launch is approximately 2.3 km and the angles α and β are both around 2.6°.

At launch, the Coriolis force is still acting on the overcarriage retarding the spring back of the ribbon. The mass of the overcarriage can be adjusted accordingly to prevent an over stressing of the ribbon. Also, the counterweights are design to absorb some of the energy of launch. The retarding force of the overcarriage and the energy absorbed by the counterweights act together to reduce the shock in the ribbon at launch.

8. Conclusion

The original ribbon model for the second generation STLS assumes a rigid (stiff) ribbon. The material tensile strength, modulus of elasticity, and mass density of a carbon nanotube ribbon is such that the ribbon is approximately a straight line from the tower to the counterweight. Using presently available materials for a first generation STLS, the ribbon is no longer a straight line but has a definite curvature. This paper introduces a new flexible ribbon model to define the curvature of the ribbon.

An example of the launch of a 35 ton launch vehicle is presented and the dynamics of the launch is discussed. It is shown that the kinetic energy of rotation can be restored in approximately 5-6 hours. Further more, it is possible that the energy of the launch will be absorbed by the retarding force on the overcarriage and any remaining energy can be absorbed by the counterweights.

References

1. Fisher, J.F., 2011, *Space Track Launch System - Updated Oct, 2011*, www.fisherspacesystems.com

2. Fisher, J.F., 2010, Space Track Launch System – Counterweight, www.fisherspacesystems.com

3. Fisher, J.F., 2009, *Space Track Launch System - Second Stage Requirements*, www.fisherspacesystems.com

4. Fisher, J.F., 2010, *Space Track Launch System – Overcarriage*, www.fisherspacesystems.com

5. Wikipedia, 2012, en.wikipedia.org/wiki/G-force, access date 02/23/2012

6. de Vries, J. 2006, *Space Elevator - Design Synthesis Exercise 2005*, Delft University of Technology, p. 44

Fisher Space Systems, LLC

Appendix A

Flexible Ribbon Model

Rad =	9.79E+04
Mcw =	3.50E+04
G =	9.81
Omg =	2.95E-02
Sig =	1.14E+09
DelL =	100
Rho =	970
Twr Ht =	8.07E+04

=B20*C20

=D20/C20

=twr+dell*COS(H20*3.1415/1

=I20*dell*Rho

=G20/sig

=ACOS(C20*g/G20)*180/3.1416

=SQRT((C20*g)^2+D20^2*omg^4)

=0.5*E20*omg^2

=C20*B20^2

=B20*C20

Rib Length	Radius	Rib Mass	Mass x Rad	Mass x Rad2	KER	Tension Sum	Theta	Area	Seg Mass	Twr Ht	Rad to CM
1.00E+05	9.79E+04	3.50E+04	3.43E+09	3.35E+14	1.46E+11	3.00E+06	83.43	2.63E-03	2.55E+02	8.07E+04	9.79E+04
9.99E+04	9.78E+04	3.53E+04	3.45E+09	3.38E+14	1.47E+11	3.02E+06	83.43	2.65E-03	2.57E+02	8.07E+04	9.79E+04
9.98E+04	9.77E+04	3.55E+04	3.48E+09	3.40E+14	1.48E+11	3.04E+06	83.43	2.67E-03	2.59E+02	8.07E+04	9.79E+04
6.00E+02	5.88E+02	4.53E+06	1.29E+11	5.75E+15	2.50E+12	1.21E+08	68.40	1.06E-01	1.03E+04	9.98E+04	2.85E+04
5.00E+02	4.95E+02	4.54E+06	1.29E+11	5.75E+15	2.50E+12	1.21E+08	68.35	1.06E-01	1.03E+04	9.98E+04	2.84E+04
4.00E+02	4.02E+02	4.55E+06	1.29E+11	5.75E+15	2.50E+12	1.21E+08	68.31	1.06E-01	1.03E+04	9.98E+04	2.83E+04
3.00E+02	3.09E+02	4.56E+06	1.29E+11	5.75E+15	2.50E+12	1.21E+08	68.26	1.06E-01	1.03E+04	9.99E+04	2.83E+04
2.00E+02	2.16E+02	4.57E+06	1.29E+11	5.75E+15	2.50E+12	1.21E+08	68.22	1.06E-01	1.03E+04	9.99E+04	2.82E+04
1.00E+02	1.23E+02	4.58E+06	1.29E+11	5.75E+15	2.50E+12	1.21E+08	68.18	1.06E-01	1.03E+04	9.99E+04	2.81E+04
0.00E+00	3.02E+01	4.59E+06	1.29E+11	5.75E+15	2.50E+12	1.21E+08	68.13	1.06E-01	1.03E+04	1.00E+05	2.81E+04

Launch Velocity and Acceleration

SQRT(9.5^2+(omg^2*A21)^2+(2*omg*E21)^2)

=SQRT(E21^2+G21^2)

omg*A21

=F21+(E22-E21)/D22

SQRT(E21^2+2*D22*dell)

(9.5*COS(C21))+(omg^2*A21*SIN(C21))

Radius	Theta (deg)	Theta (rad)	Radial Acc.	Radial Vel	Time (sec)	Tang Vel	Launch Vel	Total Acc.
3.02E+01	6.81E+01	1.19	3.56	2.67E+01	7	8.90E-01	27	9.6
1.23E+02	6.82E+01	1.19	3.63	3.79E+01	11	3.63E+00	38	9.8
2.16E+02	6.82E+01	1.19	3.70	4.67E+01	13	6.37E+00	47	9.9
4.73E+04	8.00E+01	1.40	42.15	1.48E+03	115	1.39E+03	2031	96.9
4.74E+04	8.00E+01	1.40	42.23	1.48E+03	115	1.40E+03	2035	97.0
4.75E+04	8.00E+01	1.40	42.32	1.48E+03	115	1.40E+03	2039	97.2
4.76E+04	8.01E+01	1.40	42.40	1.49E+03	115	1.40E+03	2044	97.4
4.76E+04	8.01E+01	1.40	42.48	1.49E+03	115	1.41E+03	2048	97.6
4.77E+04	8.01E+01	1.40	42.57	1.49E+03	115	1.41E+03	2052	97.8
4.78E+04	8.01E+01	1.40	42.65	1.49E+03	115	1.41E+03	2056	98.0